Histol Histopathol (2003) 18: 153-163

http://www.hh.um.es

Histology and Histopathology

Cellular and Molecular Biology

Angiogenesis after sintered bone implantation in rat parietal bone

S. Ohtsubo, M. Matsuda and M. Takekawa

Department of Oral and Maxillofacial Surgery, Asahikawa Medical College, Asahikawa, Japan

Summary. We studied the effect of bone substitutes on revascularization and the restart of blood supply after sintered bone implantation in comparison with synthetic hydroxyapatite implantation and fresh autogenous bone transplantation (control) in rat parietal bones. Methods for the study included the microvascular corrosion cast method and immunohistochemical techniques were also used.

The revascularization of the control group was the same as that for usual wound healing in the observations of the microvascular corrosion casts. The sintered bone implantation group was quite similar to that of the control group. In the synthetic hydroxyapatite group, immature newly-formed blood vessels existed even on the 21st day after implantation and the physiological process of angiogenesis was interrupted.

Immunohistochemically, vascular endothelial growth factor (VEGF), which activates angiogenesis, appeared at the early stages of both the control group and the sintered bone implantation group. VEGF reduced parallel with the appearance of the transforming growth factor factor-beta-1 (TGF-beta-1), which obstructs angiogenesis, and the angiogenesis passed gradually into the mature stage. In the hydroxyapatite implantation group, TGF-beta-1 appeared at the early stage of the implants. The appearance of VEGF lagged and it existed around the pores of hydroxyapatite even on the 21st day of the implantation. Proliferation and wandering of endothelial cells continued without any maturing of the vessels.

These findings suggest that the structure and the components of the implant material affect angiogenesis after implantation as well as new bone formation.

Key words: Angiogenesis, Microvascular corrosion cast, VEGF, TGF-beta-1, Sintered bone implantation

Offprint requests to: Dr. Seiji Ohtsubo, Department of Oral and Maxillofacial Surgery, Asahikawa Medical College, 2-1-1-1 Midorigaoka Higashi, Asahikawa, 078-8510 Japan. Fax: 0166-68-2267. e-mail: ohtsubo@asahikawa-med.ac.jp

Introduction

Sintered bone is a bone implant material obtained from natural bone tissue. The material retains bone minerals and structure in a natural form, and it does not cause an immunoreaction because it does not contain any organic components. It has been reported that the material is an excellent bone substitute with biocompatibility and osteoinductive ability when compared with other bone substitutes (Ueno et al., 1987; Yoshida et al., 1998). Scanning electron and light microscopic observations have shown that new bone adheres to sintered bone without the intervention of any fibrous tissue, which is observed with synthetic hydroxyapatite implants and that new bone invades into the sintered bone during the early stage of implantation (Matsuda et al., 1995). Furthermore, scanning electron microscope findings have shown depressed areas on the sintered bone surface just like the resorbing surface in physiological bone. This suggested that sintered bone was replaced with newly-formed bone from the host bone. We speculated that these findings would result in excellent revascularization after sintered bone implantation.

In bone healing after transplantation, revascularization in the transplanted area is very important for new bone formation and bone resorption. It is thought that natural bone spaces for bone marrow and blood vessels remain after sintering, which is different from that of synthetic hydroxyapatite. Sintered bone provides an advantageous environment for revascularization and ingrowth after implantation. Presently there are no reports on revascularization after sintered bone implantation.

In this paper, we shall present in detail the revascularization after sintered bone implantation in comparison with that of synthetic hydroxyapatite implantation and fresh autogenous bone transplantation. As methods to examine this, scanning electron microscopy for the observation of the microvascular corrosion casts as well as conventional light microscopy and immunohistochemical techniques were used.

Materials and methods

Animals

One hundred and twenty-one male Spraque-Dawley rats (aged 7 weeks, weighing about 150 g) were used in this study. They were fed conventional commercial food pellets (CE-2, Clea Japan. INC., Tokyo, Japan) and kept under optimum conditions (room temperature, 22 °C; Humidity, 55%; Lighting, 300-500 lux; bad smell, less than 20 ppm).

Preparation of implant materials

Parietal bones from three male Spraque-Dawley rats were used for the sintered bone. Rats were anaesthetized by intraperitoneal injection of sodium pentobarbital (40 mg/kg) and then sacrificed by transcardial perfusion with normal saline solution. For the preparation of sintered bone, the parietal bones were dissected from carvaria and then the peripheral soft tissue of the resected bones was removed. The resected bones were subsequently immersed in a mixture of 1% NaOH and H_2O_2 (1:1) for removal of proteins on the bone surface (room temperature, 3 hours). The first sintering was carried out by using an electric furnace (Automatic Precision Maffle Furnace, Thomas Scientific Co., Ltd. Tokyo Japan) at 600 °C for 4 hours, the subsequent second sintering was performed at 1100 °C for 3 hours, and then they were cooled at room temperature. The sintered bone was cut to a defined size (1.6x2.6 mm) and preserved at 4 °C. For the comparative study, synthetic hydroxyapatite (APACERAM, porous and dense type, pore size: from 100 μm to 245 μm, Asahi Optics INC, Tokyo, Japan) was used.

Fresh autogenous parietal bone transplantation was performed as a control in this study. For each implantation group 36 rats were used, respectively.

Transplant procedures and tissue preparations

The rats were anaesthetized by intraperitoneal injection of sodium pentobarbital (40 mg/kg), and their parietal bones were exposed by ablation of the periosteum through a dermal incision. The implant site, measuring approximately 1.6x2.6 mm, was made with the utmost care on the parietal bone using a dental bur mounted on a low-speed dental drill to avoid perforation of the dura mater. During bone resection, the surgical field was continuously irrigated with sterile saline solution to reduce thermal damage. The sintered bone, the synthetic hydroxyapatite or fresh autogenous parietal bone were implanted in the respective implant site of each parietal bone and the site was then closed by skin sutures.

The animals were divided into four groups of 36 rats for each implantation group (twelve rats were for scanning electron microscopic observation, eight rats were for light microscopy and 16 were for immunohistochemical study), and another seven rats were used for the observation of resin replica of the blood vessels without any implantation. At 4, 7, 14 and 21 days after implantation, animals of each group were anaesthetized by intraperitoneal injection of sodium pentobarbital.

For the microvascular corrosion cast under a scanning electron microscope, a cannula was introduced into the aorta, and the vasculature was perfused immediately with 50 ml of physiological saline solution and subsequently 20 ml of Mercox Resin (CL-2R-5, Dai-Nippon Ink Co. LTD., Japan) was injected with manual pressure. The corpses were kept for one hour after resin perfusion at room temperature for the polymerization and then they were immersed in a hot water bath (60 °C) to complete polymerization. The parietal bone was dissected as a sample, and then the organic substances of the specimens were dissolved by 5% sodium hypochloride for 30 minutes at room temperature. After dissolution, the microvascular corrosion cast was carefully rinsed in distilled water, and then postfixed in a 1% osmium tetroxide solution in 0.1 mol/l phosphate buffer solution (PBS) (pH 7.4) for 60 minutes. The samples were dehydrated by a graded series of ethanol. After immersion in t-butyl alcohol, they were dried in a freeze-drier (ID-2, Eiko Engineering Co.Ltd., Mito, Japan) for 12 hours. The specimens were mounted on stubs, coated by gold platinum in a vacuum device and observed with a scanning electron microscope (S-4000, Hitachi, Co. Ltd. Yokyo, Japan).

For light microscopic observation, the animals were sacrificed after anesthesia by transcardial perfusion followed by fixation in 1.25% glutaraldehyde and 4% paraformaldehyde in 0.1 mol/l PBS (pH 7.4) for 20 minutes at room temperature. The implanted areas with peripheral host bone and soft tissue were removed. The specimens were rinsed in 0.05 mol/l PBS (pH 7.4) 3 times. They were then decalcified in 10% ethylendiamine tetraacetic acid (EDTA) at room temperature for 4 days. Following this, they were embedded in glycolmethacrylate (GMA) and 3 μm-thick serial sections were made. The sections were stained with hematoxylin and eosin, and observed by conventional light microscopy.

For immunohistochemical staining, the animals were sacrificed after anesthesia by transcardial perfusion followed by fixation in 4% paraformaldehyde in 0.1 mol/l PBS (pH 7.4). After decalcification by 10 % EDTA at room temperature for ten days, the samples were embedded in paraffin.

5 μm-thick serial sections were made and deparaffinized. These samples were used for immunohistochemical staining of vascular endothelial growth factor (VEGF) and transforming growth factor-beta-1 (TGF-beta-1) (Santa Cruz Biotechnology). The sections were treated with avidin-biotin complex (Vectastain ABC kit, Vector Laboratories). They were initially treated with 0.3 % H_2O_2 for 30 minutes to inhibit endogenous peroxidase. After washing three

times in PBS (pH 7.4), they were blocked in normal goat serum for 1 hour at room temperature. They were washed in PBS (pH 7.4) three times and then incubated in primary antibody (VEGF; rabbit polyclonal IgG; diluted 1:200 in the blocking solution; Santa Cruz Biotechnology and TGF-beta-1; rabbit polyclonal IgG; diluted 1:200 in the blocking solution; Santa Cruz Biotechnology) for 2 hours at room temperature. The control sections were incubated in normal rabbit IgG. The sections were rinsed with PBS (pH 7.4) three times and incubated in biotinylated goat anti-rabbit immunoglobulin (Vector laboratories) for 30 minutes at room temperature. After washing in PBS (pH 7.4) three times, the sections were treated with avidin-biotin complex (Vectastain ABC kit, Vector laboratories) for 30 minutes. The sections were washed in PBS (pH 7.4) and then they were incubated in duraminobendigine (DAB) for 10 minutes. The sections were dehydrated in a graded series of ethanol, cleared in xylene, and mounted. The sections were counterstained with Harris' hematoxylin, and observed by a conventional light microscope.

Results

Scanning electron microscope observations

Control (Fresh autogenous bone transplantation)

Four days after transplantation, there were a few newly-formed blood vessels on the skin side. The resin replicas of the spherical or stick-like- shaped new blood vessels (diameters: from 10 μm to 15 μm) and the leakages of the resin were seen in the junction of the host and the transplanted bone. There was no new bone formation. On the dura mater side, there was a network of new blood vessels (diameter: about 7.5 μm) that originated from pre-existing blood vessels in the junction. The appearance of the vessels showed stick-like, spherical or flat shapes. There were no newly-formed blood vessels on the transplanted bone, but blood vessels (diameter: 10 μm) invaded into the transplanted bone. Spongy-like new bone formed around the newly-formed blood vessels. Seven days after transplantation, some of the new blood vessels (diameter: from 15 μm to 30 μm) and shaped like sticks in the junctions had matured and had fused. On the host bone surface, newly-formed spongy-like bone was seen around the new vessels. Bone resorption, which was seen as a

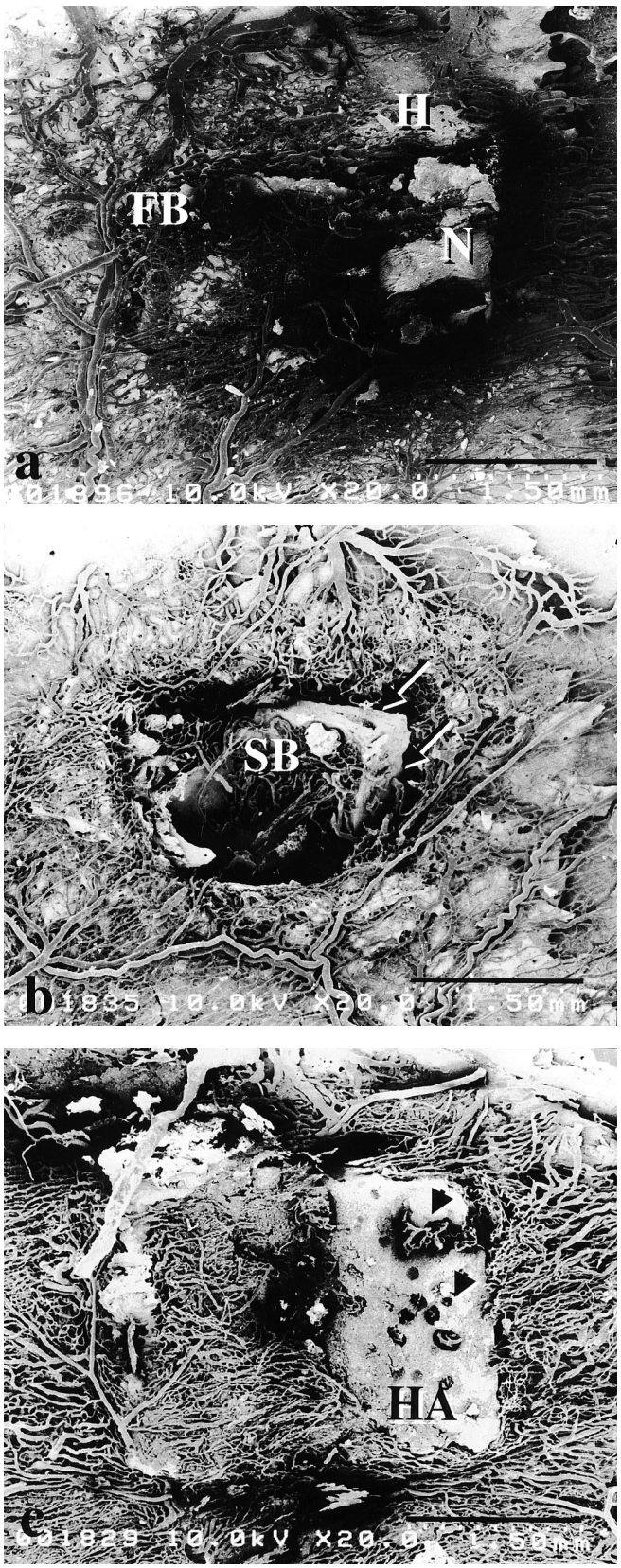

Fig. 1. SEM of vascular corrosion casts 7 days after transplantation or implantation. **a.** Fresh autogenous bone (FB): Matured and fused stick-like-shaped new blood vessels are seen in the junction of host and FB. The newly-formed bone (N) is seen around the new vessels on the host bone (H) surface. **b.** Sintered bone (SB): Shows a dense network of the new blood vessels. New vessels invade into the SB (arrows). **c.** Synthetic Hydroxyapatite (HA): Stick-like-shaped blood vessels invade into the pores of the HA (arrowheads). Bars: 1.5 mm.

continuous circle-like shape under the scanning electron microscope, was also observed on the host bone. On the dura mater side, the formation of spherical-shaped new blood vessels decreased. The newly-formed blood vessels fused with each other and /or forked into several branches. The new blood vessels were surrounded by spongy-like new bone. Fourteen days after transplantation, the new bone around the new blood vessels matured and connected the host and transplanted bone at their junction. The newly-formed blood vessels, on the dura mater side, matured with equal diameters and made a network of blood vessels on the newly-formed bone. Many new blood vessels invaded into the transplanted bone. At 21 days, the number of the blood vessels, 15 μm to 30 μm in diameter, decreased. The transplanted bone was surrounded by matured new bone on the skin side. The new bone on the dura mater side had matured completely and the number of newly-formed blood vessels decreased. The blood vessels showed full development and they included an artery with a diameter of 60 μm.

Sintered bone implantation

Four days after sintered bone implantation, there were a few newly-formed blood vessels on the skin side. Stick-like-shaped new blood vessels, 10 μm in diameter, were observed in the junction of the host and the implanted bone. On the dura mater side, a network of stick-like-shaped new blood vessels, 10 μm to 15 μm in diameter, that originated from pre-existing blood vessels was seen in the junction. Uniformly-shaped blood vessels and leakages of the resin existed around the large canaliculi in the sintered bone. Spongy-like new bone formed around the newly-formed blood vessels at the host bone side. Seven days after implantation, on the skin side, the diameter of the new blood vessels gradually increased from 15 μm to 30 μm. Fusion of the vessels and irregular arrangement were observed, but the number of blood vessels was still few. There was no invasion of the blood vessels into the sintered bone and no new bone formation. On the dura mater side, the network of the newly-formed blood vessels became denser than that of 4 days after implantation. The diameter of the new blood vessels on the implanted bone was relatively thick, in the range from 15 μm to 45 μm, and they were irregularly arranged. Some new blood

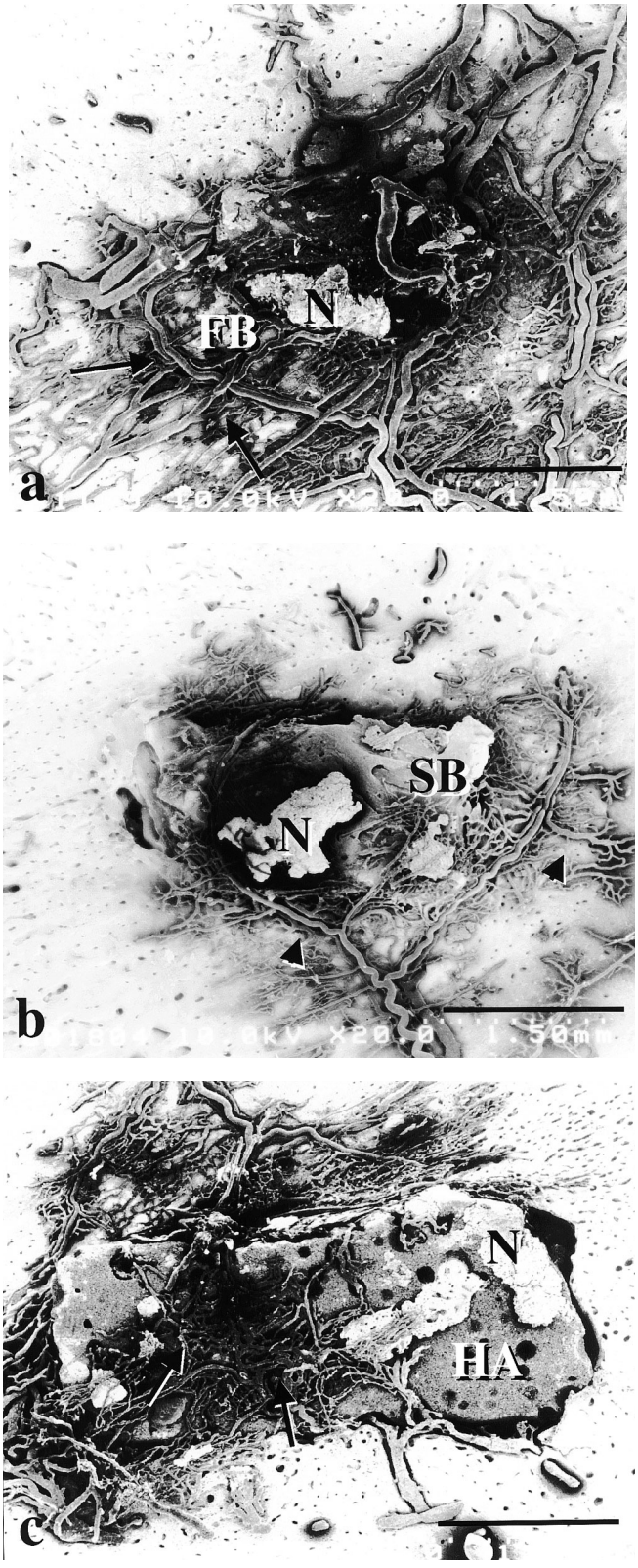

Fig. 2. SEM of vascular corrosion casts at 14 days after transplantation or implantation. **a.** Fresh autogenous bone (FB): Shows the new bone (N) around the matured new blood vessels in the junction. The new bone connects the host and the FB. The diameters of the new vessels are uniform (arrows). **b.** Sintered bone (SB): A network of new blood vessels is seen on the new bone (N) of the host side. The size of the blood vessel is uniform and the number of vessels decreases (arrowheads). **c.** Synthetic Hydroxyapatite (HA): Shows many blood vessels invaded into the pores of the HA. Spongy-like new bone (N) is seen around the new vessels and on the HA. Bars: 1.5 mm.

vessels invaded into the sintered bone. There was no bone union between the host and the implanted bone, although newly-formed bone was formed around the new blood vessels near the sintered bone in the junction. Bone resorption was observed on the host bone surface around the blood vessels. On the skin side 14 days after implantation, newly-formed blood vessels fused with a uniform thickness in the junction. New bone formation and bone resorption of the host bone were seen around the new blood vessels. The newly-formed blood vessels on the dura mater side constructed a network on the newly-formed bone. The size of the blood vessels was uniform and the number of the vessels decreased. There was a bone union between the host and the implanted bone. The implanted sintered bone was surrounded by new bone. At 21 days, the number of the blood vessels, 15 to 30 μm in diameter, decreased and the vessels developed in uniform size. An artery of 120 μm in diameter was included in the matured blood vessels. The newly-formed bone around the blood vessels matured. Bone resorption was observed on both surfaces of the host and the sintered bone. On the dura mater side, the newly-formed bone was more compact, and the number of blood vessels was extremely low.

Synthetic hydroxyapatite implantation

Four days after synthetic hydroxyapatite implantation, newly-formed blood vessels, 15 μm to 25 μm in diameter, were arranged irregularly in the junction of the host and the hydroxyapatite on the skin side. Spherical or stick-like-shaped new blood vessels, 10 μm to 15 μm in diameter, were seen around the pores of the hydroxyapatite. No blood vessels invaded into the implanted material. Resin leakage was observed on the host side. On the dura mater side, there was a network of new blood vessels, 10 μm to 15 μm in diameter, in the junction. Spherical or flat-shaped blood vessels were observed around the pores of hydroxyapatite, and spongy-like new bone was formed near the blood vessels. On the skin side, 7 days after implantation, newly-formed blood vessels were still few in number. Stick-like-shaped blood vessels, 10 to 15 μm in diameter, invaded into the relatively large pores of the hydroxyapatite (pore size: 100 μm to 150 μm in diameter). Invasion of the new blood vessels into the pores of the hydroxyapatite was observed in almost all pores (pore size: 110 μm to 245 μm in diameter) on the

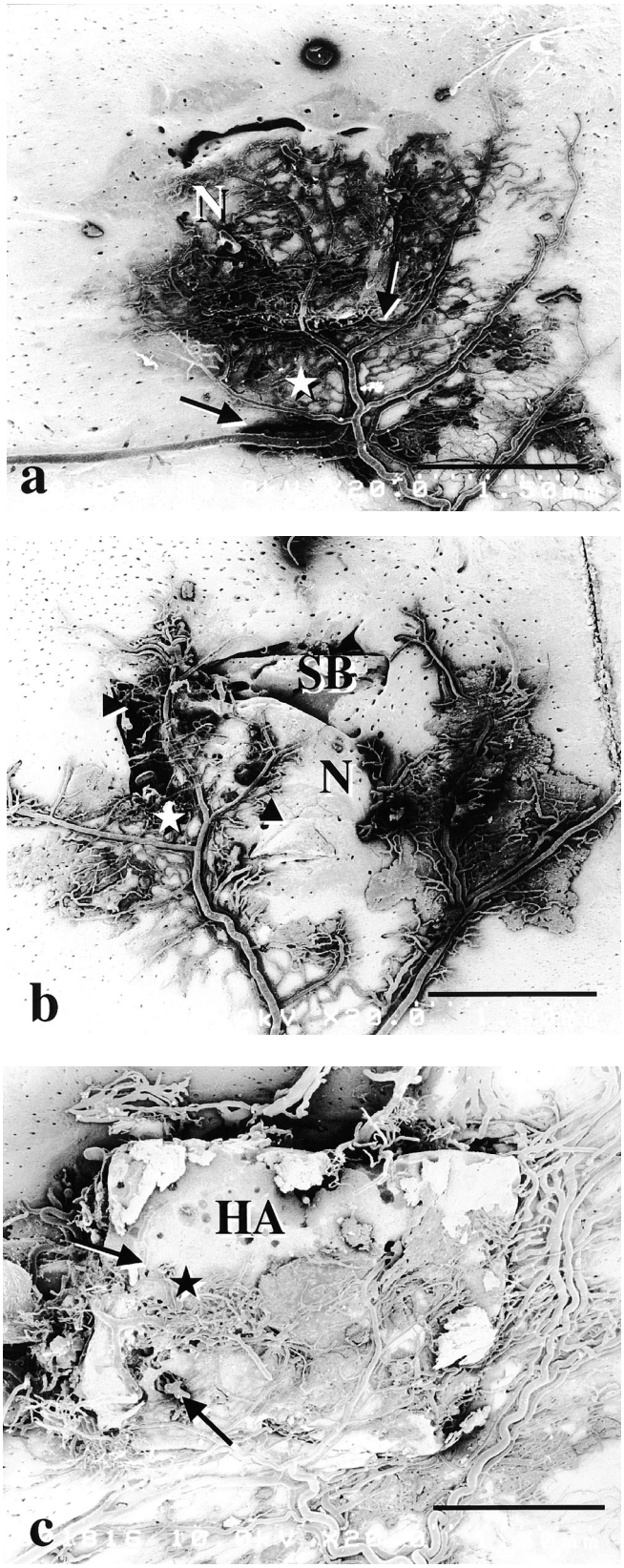

Fig. 3. SEM of vascular corrosion casts 21 days after transplantation or implantation. **a.** Fresh autogenous bone (FB): Shows a full development of new blood vessels (arrows) and the number of new vessels is decreasing. Host and transplanted FB is surrounded by matured new bone (N). **b.** Sintered bone (SB): A small number of new blood vessels with uniform size in diameter (arrowheads) are seen on the matured new bone (N) surrounding the host and implanted SB. **c.** Synthetic Hydroxyapatite (HA): Shows glomerulus-like-shaped new blood vessels (arrows) in the pores of HA. Bars: 1.5 mm.

dura mater side. On the surface of the hydroxyapatite, new blood vessels (diameter: 7.5 μm to 15 μm) originated from pre-existing blood vessels (diameter: 40 μm) and extended perpendicular to the original vessels with the fusion of the new vessels. Spongy-like new bone was formed around the blood vessels on the host and the hydroxyapatite surfaces. Fourteen days after implantation, stick-like-shaped blood vessels (diameter: 15 μm to 30 μm) and leakage of the resin were still observed in the junction. There were many blood vessels which had invaded into the pores of the hydroxyapatite. On the dura mater side, spongy-like new bone formed around the new blood vessels and on the surface of the hydroxyapatite. The number of the blood vessels that were observed on the surface of hydroxyapatite and in the junction decreased. Blood vessels with various sizes (9 μm to 40 μm in diameter) invaded into the pores of the hydroxyapatite. These new blood vessels among the new bone were in the process of maturing but immature blood vessels still existed. Twenty-one days after implantation, on the skin side, the new blood vessels fused on the hydroxyapatite and made a network of vessels. This network was looser than that of the control or the sintered bone implantation. There were glomerulus-like-shaped newly-formed blood vessels in the pores of the hydroxyapatite. On the dura mater side, the newly-formed blood vessels in the junction of the host and the hydroxyapatite had matured, but immature blood vessels still existed.

Light microscope and Immunohistochemical observations

Control (Fresh autogenous bone transplantation)

At light microscopic observation 4 days after transplantation, new bone formation was observed around the pre-existing blood vessels. There were no newly-formed blood vessels. With immunohistochemical staining, the cells around the transplanted bone showed negative immunoreaction to both VEGF and TGF-beta-1 antibodies. Seven days after transplantation, there were many newly-formed blood vessels in the junction of the host and the transplanted bone on the dura mater side. These newly-formed blood vessels were observed within the transplanted bone. Newly-formed bone was seen on the host and the transplanted bone. Immunohistochemically, many VEGF-positive cells existed in the junction, but TGF-beta-1-positive cells were few round the newly-formed bone, there were cells which showed positive immunoreaction to VEGF or TGF-beta-1. Light microscopy 14 days after transplantation showed a decrease in the number of blood vessels, and the sizes of the vessels on the dura mater side showed maturation. The newly-formed trabecular bone became thicker and more compact, and bone union by the newly-formed bone was observed between the host and the transplanted bone. It was difficult to draw a clear line between these two. Osteoclasts existed in the junction.

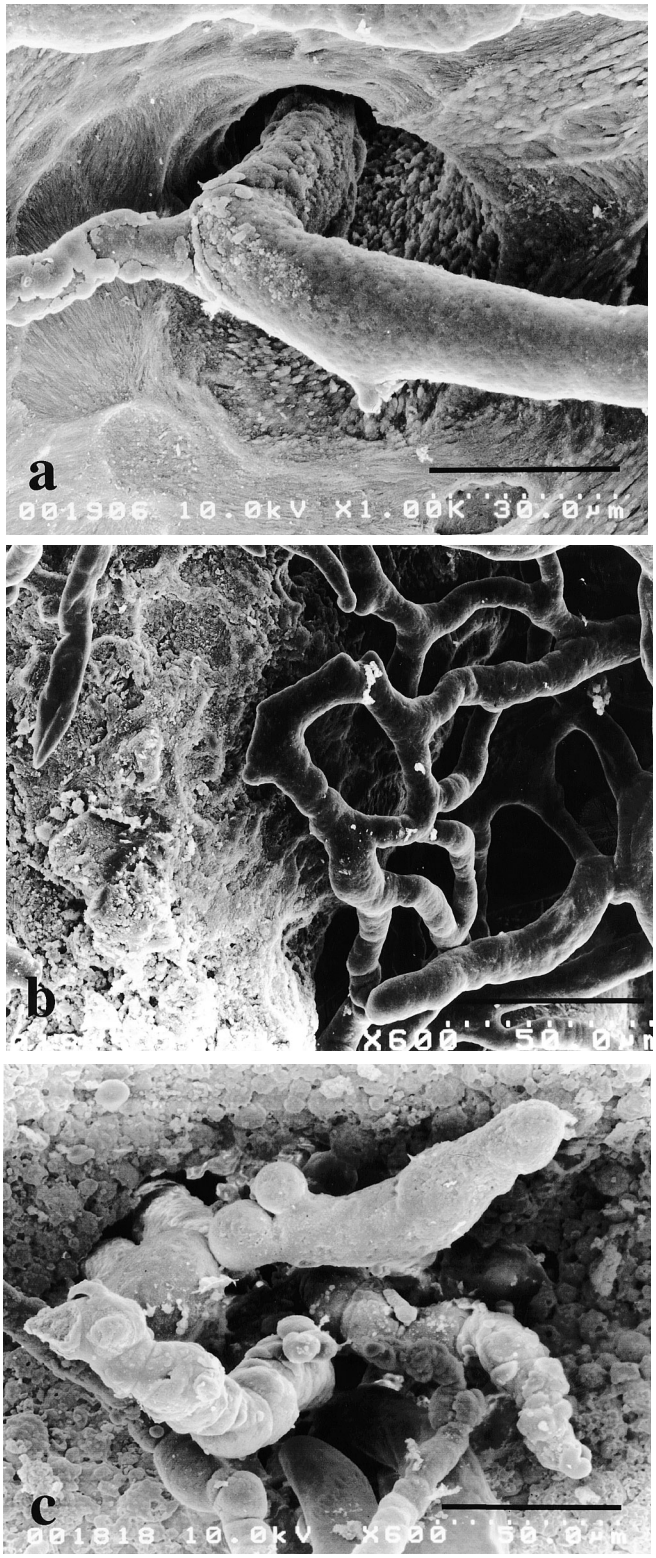

Fig. 4. High magnification of asterisk in Fig. 3a, b, c. **a.** Fresh autogenous bone. Shows a high magnification of full development of the new blood vessels at 21 days after transplantation. **b.** Sintered bone implantation. **c.** Synthetic Hydroxyapatite implantation. Bars: a, 30 μm; b, c, 50 μm.

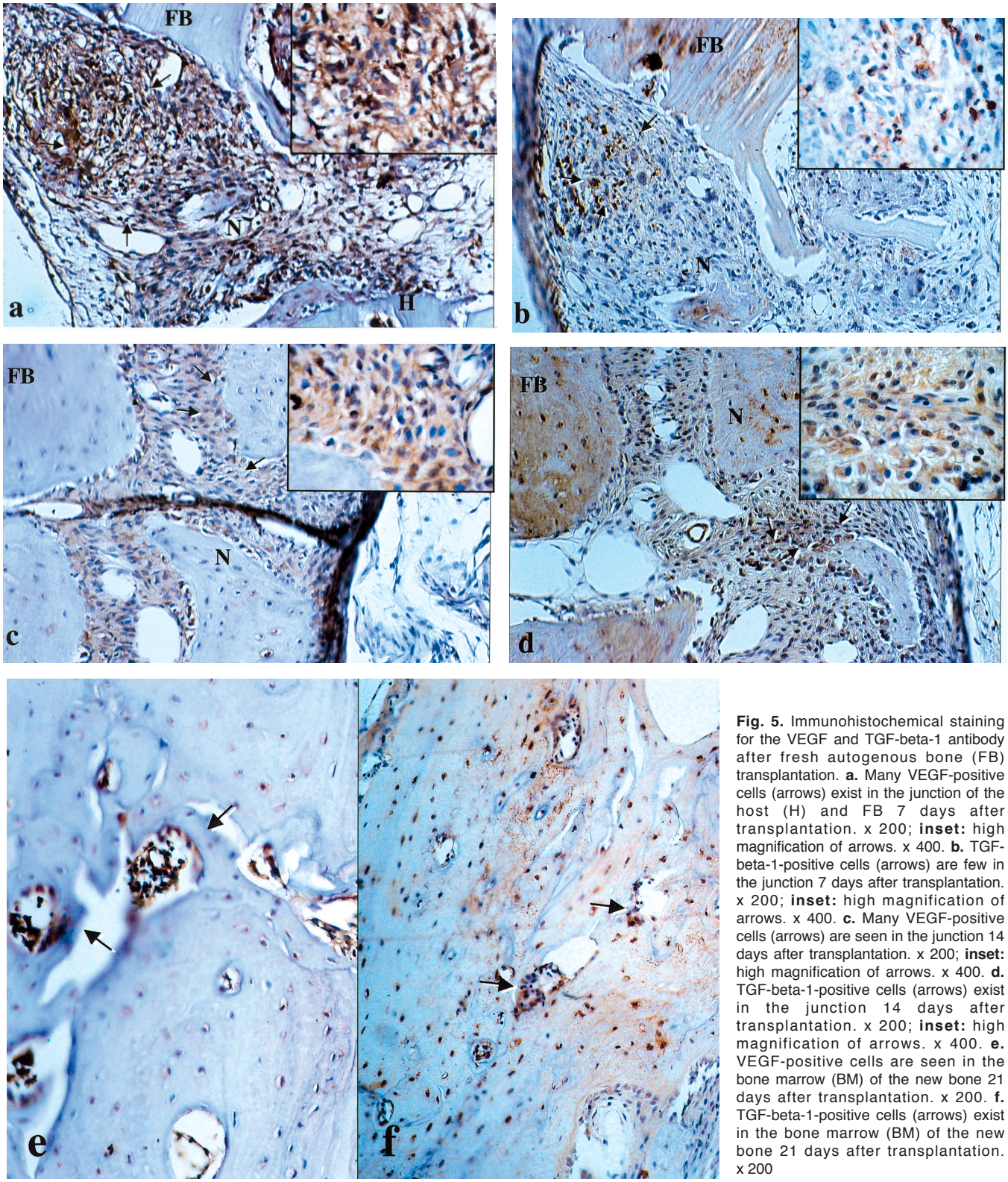

Fig. 5. Immunohistochemical staining for the VEGF and TGF-beta-1 antibody after fresh autogenous bone (FB) transplantation. **a.** Many VEGF-positive cells (arrows) exist in the junction of the host (H) and FB 7 days after transplantation. x 200; **inset:** high magnification of arrows. x 400. **b.** TGF-beta-1-positive cells (arrows) are few in the junction 7 days after transplantation. x 200; **inset:** high magnification of arrows. x 400. **c.** Many VEGF-positive cells (arrows) are seen in the junction 14 days after transplantation. x 200; **inset:** high magnification of arrows. x 400. **d.** TGF-beta-1-positive cells (arrows) exist in the junction 14 days after transplantation. x 200; **inset:** high magnification of arrows. x 400. **e.** VEGF-positive cells are seen in the bone marrow (BM) of the new bone 21 days after transplantation. x 200. **f.** TGF-beta-1-positive cells (arrows) exist in the bone marrow (BM) of the new bone 21 days after transplantation. x 200

Immunohistochemically, many VEGF-positive and TGF-beta-1-positive cells were observed in the junction. These positive cells also existed around the host and the new bone. These osteoclasts showed positive immunoreaction to both antibodies. Tweny-one days after transplantation, the number of blood vessels decreased and they had a uniform thickness on the dura mater side. The new bone matured and was surrounded

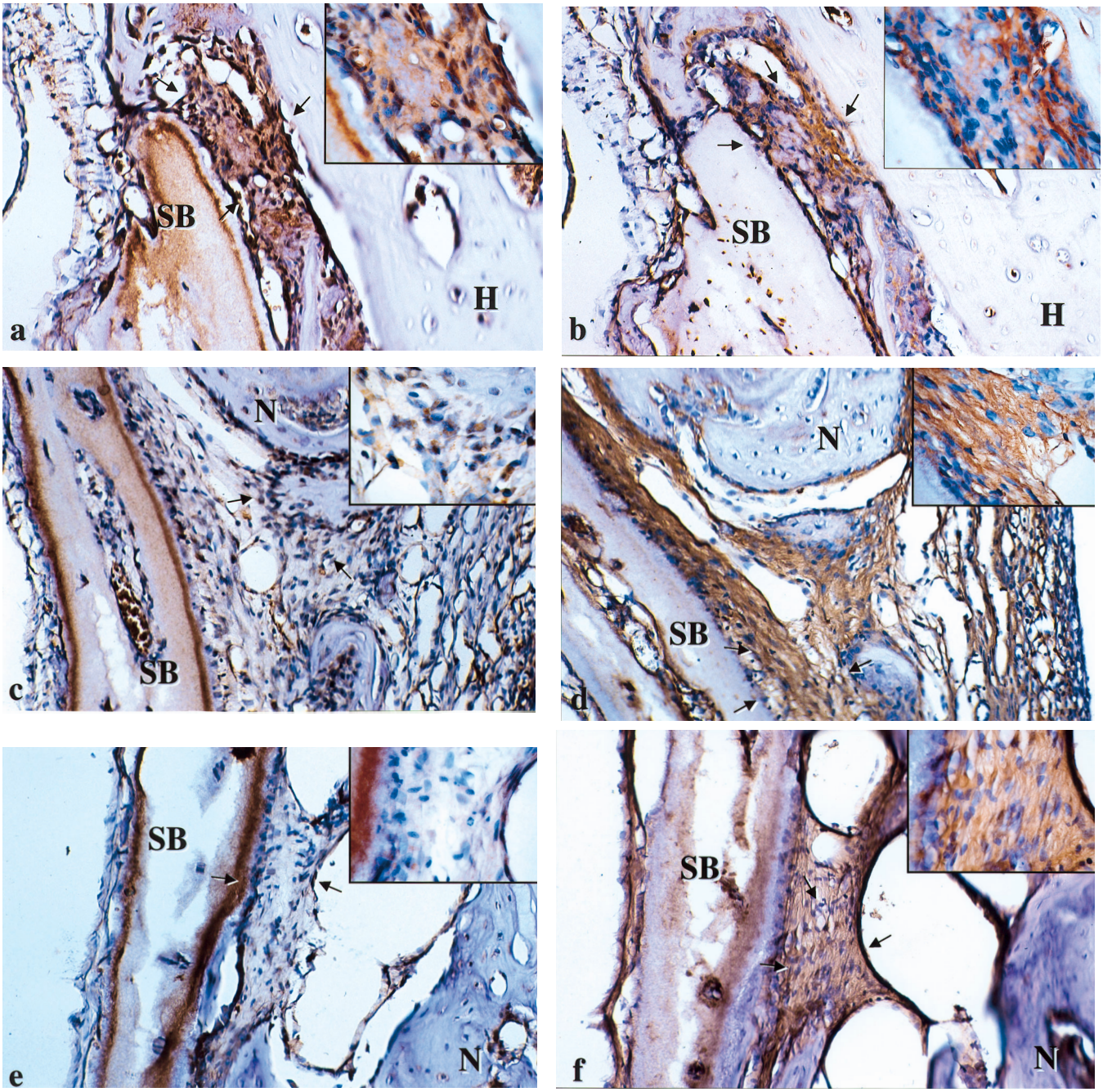

Fig. 6. Immunohistochemical staining after sintered bone (SB) implantation. **a.** Many VEGF-positive cells (arrows) are seen in the junction of the host (H) and SB 7 days after implantation. x 200; **inset:** high magnification of arrows. x 400. **b.** TGF-beta-1-positive cells (arrows) are seen in a part of the junction 7 days after implantation. x 200; **inset:** high magnification of arrows. x 400. **c.** Many VEGF-positive cells (arrows) exist in the junction 14 days after implantation. x 200; **inset:** high magnification of arrows. x 400. **d.** TGF-beta-1-positive cells (arrows) exist in the junction 14 days after implantation. x 200; **inset:** high magnification of arrows. x 400. **e.** The VEGF-positive cells (arrows) are scattered in a part of the junction 21 days after implantation. x 200; **inset:** high magnification of arrows. x 400. **f.** TGF-beta-1-positive cells (arrows) are seen in the junction. x 200; **inset:** high magnification of arrows. x 400. Cells decrease 21 days after implantation.

by flat osteoblasts. Immunohistochemical observation showed VEGF-positive and TGF-beta-1-positive cells in the bone marrow of the new bone. The number of the positive cells had decreased.

Sintered bone implantation

Light microscope observation 4 days after implantation showed no newly-formed blood vessels. New bone formation was observed around the pre-existing blood vessels on the dura mater side. Immunohistochemical staining revealed that the cells around the implanted bone were negative to both VEGF and TGF-beta-1 antibodies. Seven days after implantation, there were many newly-formed blood vessels and undifferentiated mesenchymal cells in the junction of the host and the implanted bone on the dura mater side. Newly-formed bone, constructed from thin trabecular bone with many newly-formed blood vessels, was seen on the host side. There were no new blood vessels on the skin side. Newly-formed blood vessels were seen in the sintered bone. Newly-formed bone, surrounded by osteoblasts, was observed around the newly-formed blood vessels. Immunohistochemically, many VEGF-positive cells were seen in the junction and TGF-beta-1-positive cells were scattered in the junction. Around the newly-formed bone, there were cells which showed positive immunoreaction to VEGF or TGF-beta-1. Light microscopy 14 days after implantation showed maturity of the blood vessels with a decrease in the number of new blood vessels on the dura mater side. There were no newly-formed blood vessels on the skin side. The new trabecular bone became thicker and more compact. It was difficult to distinguish the border between the host bone and the newly-formed bone. There was no new bone formation on the implanted sintered bone. Osteoclasts were seen around the implanted bone. Immunohistochemically, many VEGF-positive and TGF-beta-1-positive cells were observed in the junction. Twenty-one days after implantation, the number of blood vessels decreased but the vessels were still unequal in size on the dura mater side. The new bone had matured and was surrounded by flat osteoblasts. There were many osteoclasts around the blood vessels on the surface and inside the sintered bone. Immunohistochemically, TGF-beta-1-positive cells were still seen in the junction, but the number of immunoreactive cells had decreased. VEGF-positive cells were scattered in a part of the junction.

Synthetic hydroxyapatite implantation

Light microscopy 4 days after synthetic hydroxyapatite (HA) implantation showed no newly-formed blood vessels around the HA. New bone formation was observed around the pre-existing blood vessels on the dura mater side. Immunohistochemically, the cells around the HA showed negative immunoreaction to both VEGF and TGF-beta-1 antibodies. Seven days after implantation, there were many newly-formed blood vessels and undifferentiated mesenchymal cells in the junction of the host bone and the HA on the dura mater side. The newly-formed bone constructed from thin trabecular bone with many newly-formed blood vessels was seen on the host bone. Osteoclasts were scattered in the junction of the host and the HA. Newly-formed blood vessels and many undifferentiated mesenchymal cells were seen in the pores of the HA. In immunohistochemical staining, VEGF-positive and TGF-beta-1-positive cells were observed in the junction, in the endothelial cells of the blood vessels and around the newly-formed bone and in the pores of the HA. Fourteen days after implantation, there were few blood vessels and no new bone formation on the HA. Newly-formed blood vessels were seen in a part of the pores of the HA. Immunohistochemically, many VEGF-positive cells were observed in the junction and in the pores of the HA. TGF-beta-1-positive cells decreased in number in comparison with that of 7 days. Around the newly-formed bone and the host bone, VEGF-positive and TGF- beta-1-positive cells were observed. Osteoclasts showed positive immunoreaction to both antibodies. Twenty-one days after implantation, there were many unequal-sized blood vessels on the dura mater side. Newly-formed bone and newly-formed blood vessels were observed in a part of the pores of HA, but they were still immature. Immunohistochemically, VEGF-positive and TGF-beta-1-positive cells were seen in the junction and in the osteoclasts. The VEGF-positive cells still existed in and around the pores of the HA.

Discussion

Generally, revascularization in wound healing shows the process of angiogenesis, which is the formation of new capillary blood vessels from existent microvessels by sprouting from endothelial cells (Risau and Flamme, 1995). With the scanning electron microscope and the light microscope in this study, it was clear that revascularization after autogenous bone transplantation (control) was the same process as in usual wound healing.

In sintered bone implantation, the process of revascularization was quite similar to that of the control in morphology and in its temporal course. With synthetic hydroxyapatite, however, immature newly-formed blood vessels still existed in the pores of hydroxyapatite even 21 days after implantation and the usual process of angiogenesis was interrupted. A comparative study using a scanning electron microscope of the healing processes of the sintered bone implantation and the synthetic hydroxyapatite implantation concluded that the natural structure of the sintered bone had a good effect on the tissue reaction after the implantation (Matsuda et al., 1995). It has also been said that the natural multiple porous structure of the fresh autogenous bone and sintered bone is good for cell attachment to the implant

(Tatsumi et al., 1988). In this study, it was suggested that the structure of the implant material that is endowed by nature, affects new bone formation and angiogenesis after implantation. Perhaps this plays an important role in the incorporation of implants.

Angiogenesis is induced by many mediators, like

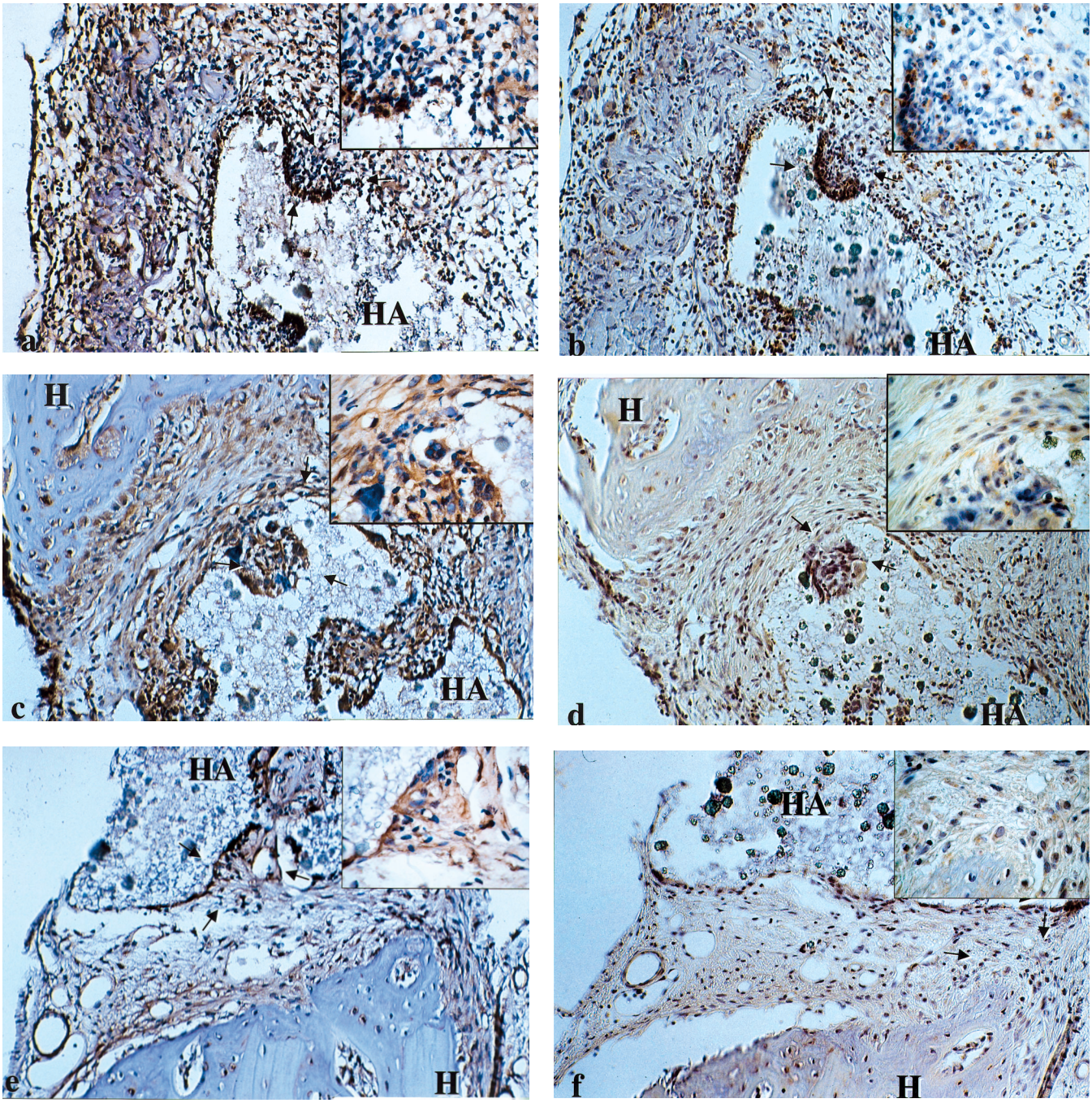

Fig. 7. Immunohistochemical staining after synthetic hydroxyapatite (HA) implantation. **a.** VEGF-positive cells (arrows) exist in the junction of the host and HA 7 days after implantation. x 200; **inset:** high magnification of arrows. X 400. **b.** TGF-beta-1-positive cells (arrows) are seen in the junction 7 days after implantation. x 200; **inset:** high magnification of arrows. x 400. **c.** Many VEGF-positive cells (arrows) exist in the junction and in the pores of HA at 14 days after implantation. x 200; **inset:** high magnification of arrows. x 400. **d.** TGF-beta-1-positive cells (arrows) decrease in comparison with those at 7 days. x 200; **inset:** high magnification of arrows. x 400. **e.** The VEGF-positive cells (arrows) still exist in and around the pores of HA at 21 days after implantation. x 200; **inset:** high magnification of arrows. x 400. **f.** TGF-beta-1-positive cells are seen in the junction. x 200; **inset:** high magnification of arrows. x 400

cytokines or growth factors, and is regulated strictly by the interaction of the activated factors and/or the obstructed factors. Vascular endothelial growth factor (VEGF) is a representative factor that activates angiogenesis by proliferating the vascular endothelial cells specifically (Ferrara, 2000). VEGF is regulated strictly in vivo, and a change in its quantity induces various obstacles to the vascular system (Carmelite et al., 1996). While the representative obstructed factor is a transforming growth factor beta (TGF-ß), it has an inhibitory action on the wandering of vascular endothelial cell (Alicia et al., 1989).

In autogenous bone transplantation and sintered bone implantation of the present study, VEGF appeared and induced angiogenesis at an early stage of the transplantation or the implantation. VEGF reduced parallel with the appearance of TGF-ß and the angiogenesis passed gradually into the mature stage. In hydroxyapatite implantation, TGF-ß protein appeared at the early stage of the implant. The appearance of VEGF proteins lagged and they existed around the pores even on the 21st day of the hydroxyapatite implantation. Proliferation and wandering of the endothelial cells continued without any maturing of the vessels. These results are reflected in the observations of the scanning electron microscope in this study. It is suggested that hydroxyapatite, as a bone implant material, delayed or interrupted angiogenesis after the implantation by affecting the appearance of the regulating factors for angiogenesis.

The blood vessels that can adapt to the metabolic activity of the cells are the capillaries. When the cells have lively metabolic action, dense capillary networks are formed around the cells for the nutritional supply. On the contrary, the capillary networks are rough and separate from the cells when the metabolic activity of the cells decreases (Iwaku, 1989). New bone formation of the control group and the sintered bone implantation group of this study were closely related to the angiogenesis and the resumption of blood flow after implantation. However, in the implantation of the synthetic hydroxyapatite, new bone formation was time-consuming and the process of angiogenesis was delayed. This means that the structure and the components of the implant material affected both new bone formation and angiogenesis in wound healing.

Angiogenesis and signal transduction in the microenvironment surrounding the implant material are very important for bone healing after bone transplantation or implantation because many transmitters come to the implant area through the blood flow. Chalmers et al. (1975) reported in their experimental bone formation in soft tissue that three important factors: bone inductive factor (BMP); osteogenic precursor cells; and a good environment are necessary for osteogenesis. The authors think that the condition of the bone substitute for the success of the bone implantation requires that the structure and the components of the host cells make a favorable environment for normal wound healing.

Sintered bone possesses sufficient satisfactory requirements as a bone substitute except for its weak mechanical strength. Improvement of this weakness and a molecular biological study of the microenvironment around sintered bone implants require further exploration.

Acknowledgements. The authors are grateful to Prof. Sinichi Kita, Department of Oral and Maxillofacial Surgery, Asahikawa Medical College, for his encouragement and helpful suggestions throughout the course of this work. We wish to express our thanks to Dr. Hajime Tanaka and Miss Ryoko Yamazaki, Department of Pediatrics Asahikawa Habilitation Center for Disabled Children, for their useful comments and skillful technical assistance.

References

Alicia A.O., Kim B.S., Sandra R.S. and Patricia A.D. (1989). An activated form of transforming growth factor is produced by cocultures of endothelial cells and pericytes. Proc. Natl. Acad. Sci. USA 86, 4544-4548.

Carmeliet P., Ferreira V., Breier G., Pollefeyt S., Kieckens L., Gertsenstein M., Fahrig M., Vandenhoeck A., Harpal K., Eberhardt C., Declercq C., Pawling J., Moons L., Collen D., Risau W. and Nagy A. (1996). Abnormal blood vessel development and lethality in embryos lacking a single VEGF allele. Nature 380, 435-439.

Chalmers J., Gray D.H. and Rush J. (1975). Observations on the induction of bone in soft tissues. J. Bone Joint Surg. 57-B, 36-45.

Ferrara N. (2000). Vascular endothelial growth factor and the regulation of angiogenesis. Recent. Prog. Horm. Res. 55, 15-35.

Iwaku F. (1989). Microvasculature of Bone. II. The three dimensional corrosion cast microvasculature on the outer surface of the rat's parietal bone. J. Bone Mineral Metabol. 7, 7-11.

Matsuda M., Kita S., Takekawa M., Ohtsubo S. and Tsuyama K. (1995). Scanning electron and light microscopic observations on the healing process after sintered bone implantation in rat. Histol. Histopathol. 10, 673-679.

Risau W. and Flamme I. (1995). Vasculogenesis. Annu. Rev. Cell Dev. Biol. 11, 73-91.

Tatsumi J., Kurihara N., Takahashi T., Shimoyama M., Karami K. and Ikeda K. (1988). Clinical application of sintered bone (I). Nippon Shishubyo Gakkai Kaishi. 30, 164-171.

Ueno Y., Shima Y. and Akiyama T. (1987). Development new biomaterial as a bone substitute: true bone ceramics. In: Materials science monographs, 39. Ceramics in clinical applications. Vincentini P. (ed). Proceedings of the International Symposium on Bioceramics. pp 369-378.

Yoshida T., Itoh T., Saitoh T. and Sekine I. (1998). Histopathological study of the use of freeze-dried allogenic dentin powder and true bone ceramic as apical barrier materials. J. Endod. 24, 581-586.

Accepted October 14, 2002